
Optimization of a Medium-Voltage Distribution Network via Photovoltaic Integration: A Case Study of the Liouesso MT Grid

Tite Lawd Ngouloubi*, Rodolphe Gomba, Mathurin Gogom, Nianga-Apila, Amos Omboua Eyandzi

Polytechnic Superior National School (ENSP), Marien Ngouabi University, Brazzaville, Congo

Email address:

ngouloubitite@gmail.com (Tite Lawd Ngouloubi), gombarodolphe@gmail.com (Rodolphe Gomba),

mathuringogom@gmail.com (Mathurin Gogom), apilanianga@gmail.com (Nianga-Apila), ombouaweb@gmail.com (Amos Omboua Eyandzi)

*Corresponding author

To cite this article:

Tite Lawd Ngouloubi, Rodolphe Gomba, Mathurin Gogom, Nianga-Apila, Amos Omboua Eyandzi. (2025). Optimization of a Medium-Voltage Distribution Network via Photovoltaic Integration: A Case Study of the Liouesso MT Grid. *Science Journal of Energy Engineering*, 13(3), 108-119. <https://doi.org/10.11648/j.sjee.20251303.11>

Received: 17 June 2025; **Accepted:** 30 June 2025; **Published:** 14 July 2025

Abstract: This study rigorously investigates the technical implications of integrating a 3 MW photovoltaic (PV) power plant into a real-world medium-voltage (MT) distribution network located in Liouesso, Republic of Congo. The targeted grid is characterized by a semi-urban infrastructure with limited dynamic compensation capabilities and frequent critical undervoltage conditions. Unlike many studies that rely on theoretical models or synthetic datasets, this research is grounded in actual operational measurements (load profiles, nodal voltages) and high-fidelity dynamic simulations performed using the PSAT toolbox within the MATLAB environment. Two operating scenarios are evaluated: the baseline network performance without PV injection, and a modified configuration including active solar power injection at a strategically selected node (Bus 18). The results show that such controlled integration not only improves the voltage profile eliminating undervoltages below 0.95 p.u. but also significantly reduces active line losses (by 15 to 20 %), all while complying with international power quality standards such as IEC 61000-4-30 and EN 50160. The adopted methodological approach combines topological analysis, dynamic electrotechnical modeling, and empirical data utilization, thereby offering a robust operational framework for optimal PV sizing and siting in weakly interconnected African networks. The study also highlights that these benefits are achieved without the need for costly compensation equipment such as STATCOMs or SVCs, reinforcing the economic feasibility of this solution for developing countries. Beyond its environmental merits, photovoltaic energy emerges in this context as a strategic tool for modernizing MT networks, contributing to enhanced voltage stability, improved power quality, and greater overall system resilience. This research thus provides actionable recommendations for energy planning and intelligent renewable integration strategies in African settings.

Keywords: MT Distribution Network, Photovoltaic Integration, Voltage Stability, PSAT Simulation, Real-world Network, Energy Optimization, Distributed Injection, Topological Analysis

1. Introduction

Electrical energy, a pillar of human development, requires reliable networks for its transmission. However, these networks are exposed to various disruptive phenomena losses, imbalances, surges, or dynamic instabilities that compromise their proper functioning. Electrical stability analysis aims to understand and anticipate the behaviour of the network in the

face of these disturbances, whether minor or severe [1, 2].

The global energy transition necessitates a paradigm shift in power system architecture particularly within medium-voltage (MT) networks, to meet escalating demands for reliability, energy efficiency, and sustainability. The rise of decentralized renewable energy sources, most notably solar photovoltaics (PV), is reshaping traditional paradigms of grid operation. Originally designed for unidirectional, centralized

energy flows, (MT) grids must now accommodate intermittent, bidirectional injections of unpredictable magnitude [3–5].

While environmentally and economically advantageous, PV integration introduces systemic side effects that compromise grid stability. Discontinuous active power injections may induce voltage oscillations, load imbalances, degraded power factors, and inefficient energy flow redistribution. These issues are exacerbated in rural or weakly interconnected grids, requiring meticulous evaluation to maintain power quality standards [6–8].

Much of the extant literature relies on stylized models or synthetic data, often divorced from the empirical. The academic literature is replete with modeling and simulation-based approaches for analyzing the impact of renewable energy on distribution networks. However, many such studies rely on idealized system configurations, synthetic load profiles, or benchmark networks that bear limited resemblance to the realities of developing countries. In particular, empirical analyses grounded in operational data from African networks remain scarce, thereby constraining the applicability and relevance of findings for local utility operators [9, 10].

In this context, the present study aims to rigorously assess the technical impact of a 3 MW photovoltaic unit on an existing (MT) distribution network located in Liouesso, the Republic of Congo. This network typifies a semi-urban, under-resourced configuration characterized by recurrent voltage sags. Using real-world data such as load profiles and voltage measurements, and a dynamic simulation framework developed in PSAT within the MATLAB environment, two operating scenarios are analyzed: baseline performance without solar generation, and a post-integration scenario with PV injection at a strategically selected node (Bus 18). The objective is to quantify the effects of PV integration on key performance indicators including nodal voltage, energy losses, and local stability against the benchmarks set by IEC 61000-4-30 and EN 50160 standards. Beyond its analytical dimension, this study seeks to demonstrate that photovoltaic injection, when appropriately dimensioned and optimally located, can serve as a passive yet effective voltage regulation mechanism tailored to the technical and economic realities of African (MT) networks. In doing so, it offers an operational framework to inform strategic decisions on solar plant siting in transitioning electric power systems.

2. Literature Review

The evolution of power systems toward more open and decentralized architectures has revealed new constraints related to dynamic stability and power quality, particularly within medium-voltage (MT) distribution networks. Originally designed for unidirectional power flows from centralized generation sources, these networks are now increasingly exposed to local injections whose variability and unpredictability challenge both operational balance and systemic robustness.

2.1. Stability and Quality of Energy in HTA Networks

The global transition toward decentralized electricity networks has highlighted a range of emerging challenges, particularly concerning dynamic stability and power quality. (MT) grids, originally designed for unidirectional power flow from centralized generation assets, must now accommodate local injections whose fluctuating and unpredictable nature poses significant threats to the grids operational integrity.

While photovoltaic (PV) integration offers clear environmental and economic benefits, it also induces non-negligible side effects on system stability. Intermittent active power injections may result in voltage fluctuations, load unbalancing, reduced power factors, and inefficient energy flow distribution. These issues are exacerbated in rural or weakly interconnected contexts, thereby requiring rigorous assessment to ensure alignment with established power quality standards.

Recent studies have shed light on the influence of PV integration on voltage stability. For example, Maghami *et al.* analyzed the effects of increasing PV penetration in a typical Malaysian MT distribution network using static and dynamic simulations via DIgSILENT PowerFactory [11]. Their findings revealed that, under peak load conditions, voltage violations occur at certain nodes; however, these violations diminish as PV penetration increases, ultimately converging to acceptable operational thresholds.

Similarly, a study by Moutevelis demonstrated that high penetration of renewable sources especially PV introduces challenges related to voltage deviation and system stability [12]. These include overvoltages during peak solar production, reverse power flows, and sudden voltage drops due to the inherently volatile nature of renewable energy generation.

2.2. Photovoltaic Integration into Electric Distribution Networks

Integrating photovoltaic generation into distribution networks holds significant promise for accelerating the energy transition and reducing transmission and distribution losses. However, this integration fundamentally alters power flow patterns and introduces complex dynamics, particularly within (MT) networks characterized by low load densities. Research efforts have explored a variety of mitigation strategies. A study published in Sustainability evaluated the impact of PV penetration on a Malaysian (MT) distribution grid, assessing voltage stability, power losses, and fault conditions under varying load scenarios. The findings showed that increasing PV penetration enhances voltage stability and reduces losses, although high levels of penetration may still give rise to voltage violations.

Other studies underscore the critical role of voltage regulation and coordinated control strategies. For instance Li *et al.* proposed an optimization framework to coordinate reactive power injections from smart inverters alongside tap changer operations in unbalanced, multiphase distribution networks [13]. Their approach yielded significant reductions in voltage

deviations and successfully mitigated overvoltage events. Despite these advancements, notable gaps remain particularly in translating such strategies to the specific operational and structural conditions of African networks. This study seeks to address that deficiency by proposing a hybrid methodology that combines empirical field data with realistic simulations to evaluate the impacts of PV integration on voltage stability and power quality within a real (MT) network in the Republic of Congo

3. Methodology

3.1. Modeling of the (MT) Distribution Network

The medium-voltage (MT) distribution network under investigation is located in Liouesso, Republic of the Congo. It comprises 76 interconnected buses linked primarily by underground cables of the Almelec type, with a cross sectional area of 54.6 mm^2 , operating at nominal voltages of 20 kV and 30 kV. The distribution network follows a radial topology and is supplied by a primary HT/MT substation that serves multiple semi-urban zones.

The generation sources comprising both centralized power plants and potential photovoltaic units are detailed in Table 1 (*Technical Specifications of Power Plants, Annex*), which provides the injected power values for each unit.

Inter-bus transmission lines are modeled by incorporating the geometric and electromagnetic characteristics of the cables. The calculated values of resistance r_0 and reactance x_0 , expressed in per-unit (p.u.) values, are presented in Table 2 (*Line Characteristics, Annex*).

Finally, the electrical loads encompassing both active and reactive power consumption at each bus are compiled in Table 3 (*Load Characteristics, Annex*). These datasets constitute the foundation for evaluating the overall load profile, quantifying line losses, and planning for reactive power compensation strategies[14, 15].

$$R = \rho \cdot \frac{\ell}{S} \quad (1)$$

$$X = 2\pi f \cdot L' \cdot \ell \quad (2)$$

$$B = 2\pi f \cdot C' \cdot \ell \quad (3)$$

where :

1. ρ : Electrical resistivity of the conductor material (in $\Omega \cdot \text{m}$),
2. ℓ : Length of the line (in m),
3. S : Cross-sectional area of the conductor (in m^2),
4. f : System frequency (50Hz),
5. L' : length inductance(in H/m),
6. C' : length capacitance(in F/m).

or the underground lines considered in this study, the values of L' and C' are sourced from the technical datasheets provided by the cable manufacturer. The resistivity ρ is taken to be equal to $3,32 \times 10^{-8} \Omega \cdot \text{m}$ for Almelec.

All computed parameters, initially expressed in ohms or

siemens, are subsequently converted into per-unit (p.u.) values using a standardized base. The base impedance is defined in accordance with references[14, 15] :

$$Z_{\text{base}} = \frac{V_{\text{base}}^2}{S_{\text{base}}} \quad (4)$$

where V_{base} represents the nominal system voltage (either 20 kV ou 30 kV), and S_{base} is the reference apparent power, conventionally set at 100 MVA. The per-unit conversions are thus performed as follows:

$$R_{\text{pu}} = \frac{R}{Z_{\text{base}}}, \quad X_{\text{pu}} = \frac{X}{Z_{\text{base}}}, \quad B_{\text{pu}} = B \cdot Z_{\text{base}} \quad (5)$$

All these values are detailed in the tables provided in Annex, which include the line lengths, impedance parameters, susceptance values, and the topological layout of the entire network. The comprehensive network modeling was carried out using the Power System Analysis Toolbox *PSAT* within the *MATLAB* environment, under the assumption of a balanced steady-state sinusoidal regime.

3.2. Sizing of the Photovoltaic Power Plant

The integration of a photovoltaic power plant into the Liouesso (MT) distribution network is intended to mitigate severe voltage sags observed during peak demand periods, without relying on conventional compensation devices. The selection of a 3 MW capacity was made based on a joint evaluation of the networks energy requirements, the available voltage margins, and the hosting capacity at the designated injection point (bus 18).

3.2.1. Inverter Apparent Power

The required apparent power is calculated using the peak active power output of the PV plant, denoted P_{PV} and the minimum permissible power factor $\cos \varphi = 0,85$:

$$S = \frac{P_{PV}}{\cos \varphi} \quad (6)$$

$$S = \frac{3 \text{ MW}}{0,85} \approx 3,53 \text{ MVA} \quad (7)$$

3.2.2. Maximum Injection Current

The current injected into the MT distribution network assuming a nominal voltage ($U_n = 20 \text{ kV}$) is determined using the following relation:

$$I_{PV} = \frac{S}{\sqrt{3} \cdot U_n} \quad (8)$$

$$I_{PV} = \frac{3,53 \times 10^6}{\sqrt{3} \cdot 20 \times 10^3} \approx 102 \text{ A} \quad (9)$$

3.2.3. Estimation of the Photovoltaic Field

Assuming standard solar irradiance conditions of 1000 W/m^2 and an average panel efficiency $\eta_{PV} = 18\%$, the surface power density is calculated as:

$$P_{\text{surf}} = G \cdot \eta_{PV} = 1000 \cdot 0,18 = 180 \text{ W/m}^2 \quad (10)$$

Based on this value, the total surface area required for the photovoltaic panels to achieve a peak power output of 3 MW is:

$$S_{PV} = \frac{3 \times 10^6}{180} \approx 16\,667 \text{ m}^2 \quad (11)$$

3.2.4. Optional Storage Capacity

To compensate for short-term fluctuations, such as 30 minutes of full-power operation, an energy storage system may be considered. The required storage energy E is estimated as:

$$E = P_{PV} \cdot T = 3 \text{ MW} \cdot 0,5 \text{ h} = 1,5 \text{ MWh} \quad (12)$$

Assuming an average direct current (DC) bus voltage of 800 V, the corresponding storage capacity in ampere-hours is given by:

$$Q = \frac{E}{U} = \frac{1,5 \times 10^6}{800} = 1875 \text{ Ah} \quad (13)$$

3.2.5. Justification of the Integration Point

The selection of Bus 18 as the Integration point for the photovoltaic plant results from a detailed topological and energetic analysis of the Liouesso (MT) distribution network. In the absence of localized generation, this area exhibits significantly depressed voltage levels an indication of structural weakness and pronounced stress on the upstream feeder. Figure 1 illustrates the distribution of active (P), reactive (Q), and apparent (S) power across the networks 76 buses. A distinct, localized power injection is observed at Bus 18, contrasting sharply with the predominantly consumptive behavior of the other nodes. This imbalance renders Bus 18 strategically advantageous for several reasons:

1. It enables direct compensation of local demand, thereby reducing upstream loading;
2. It contributes to voltage profile homogenization in a historically unstable zone;
3. It mitigates Joule losses by reducing the magnitude of transmitted currents;
4. It establishes a capacitive support point through reactive power contribution from the inverter.

Injection at Bus 18 thus functions as a stabilizing lever both locally and system-wide. It enhances network stiffness while adhering to the operational constraints inherent to real-world (MT) systems, without inducing overvoltages on adjacent segments

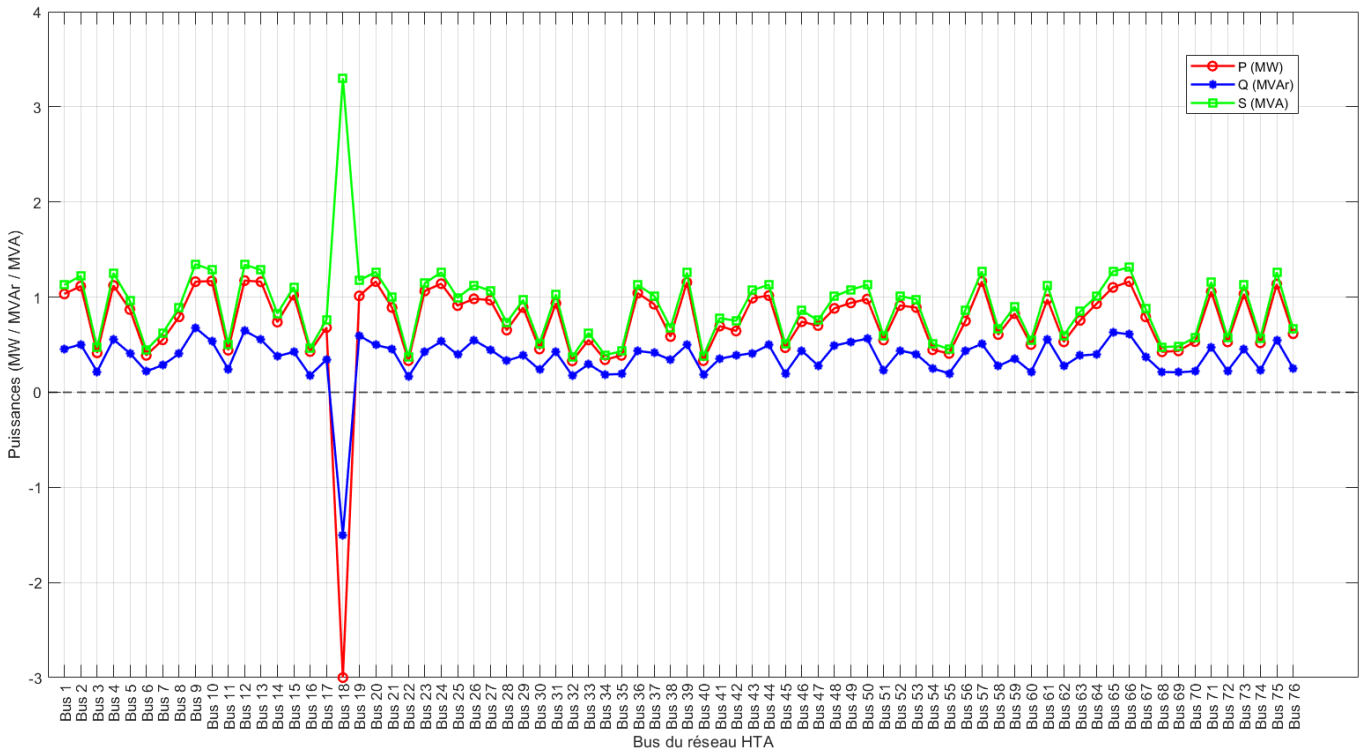


Figure 1. Power Injection and Absorption Profile Across the 76-Bus (MT) Network.

3.3. Integration of the Photovoltaic Plant

The goal is to model the temporal evolution of the complex voltage $V(t)$ at a Medium Voltage (MT) node supplied by a photovoltaic (PV) power plant. This modeling facilitates the dynamic stability analysis of the system as a function of the injected power.

1. The electrical node is modeled as an equivalent capacitance C_{eq} ;
2. The complex power resulting from the integration of the PV plant into the grid is defined as $S(t) = P(t) + jQ(t)$;

$$P(t) + jQ(t) = (V_r + jV_i)(I_r - jI_i) = (V_r I_r + V_i I_i) + j(V_i I_r - V_r I_i) \quad (15)$$

which leads to the following system:

$$\begin{cases} P = V_r I_r + V_i I_i \\ Q = V_i I_r - V_r I_i \end{cases} \quad (16)$$

Matrix form :

$$\begin{bmatrix} P \\ Q \end{bmatrix} = \begin{bmatrix} V_r & V_i \\ V_i & -V_r \end{bmatrix} \begin{bmatrix} I_r \\ I_i \end{bmatrix} \quad (17)$$

Inversion of system:

$$\begin{bmatrix} I_r \\ I_i \end{bmatrix} = \frac{1}{V_r^2 + V_i^2} \begin{bmatrix} V_r & V_i \\ V_i & -V_r \end{bmatrix} \begin{bmatrix} P \\ Q \end{bmatrix} \quad (18)$$

which leads:

$$\begin{cases} I_r = \frac{PV_r + QV_i}{V_r^2 + V_i^2} \\ I_i = \frac{PV_i - QV_r}{V_r^2 + V_i^2} \end{cases} \quad (19)$$

Based on Kirchhoffs law, the net current at the node is modeled as the current flowing through an equivalent capacitance C_{eq} :

$$I(t) = C_{eq} \cdot \frac{dV(t)}{dt} \quad (20)$$

As if the components:

$$\begin{cases} I_r = C_{eq} \cdot \frac{dV_r}{dt} \\ I_i = C_{eq} \cdot \frac{dV_i}{dt} \end{cases} \quad (21)$$

Substituting I_r and I_i :

$$\begin{cases} \frac{dV_r}{dt} = \frac{1}{C_{eq}} \cdot \frac{PV_r + QV_i}{V_r^2 + V_i^2} \\ \frac{dV_i}{dt} = \frac{1}{C_{eq}} \cdot \frac{PV_i - QV_r}{V_r^2 + V_i^2} \end{cases} \quad (22)$$

This nonlinear differential system describes the temporal evolution of the voltage at the point of common coupling (PCC) with the photovoltaic (PV) power plant. It provides a

3. The nodal voltage is expressed as: $V(t) = V_r(t) + jV_i(t)$;
4. The injected current is $I(t) = I_r(t) + jI_i(t)$.

The interplay between complex power and current is derived from the fundamental definition of complex power:

$$S(t) = V(t) \cdot I^*(t) \quad (14)$$

where $I^*(t)$ denotes the complex conjugate of the injected current. Expanding the product yields:

foundational framework for:

1. Analyzing transient voltage responses under disturbances;
2. Evaluating the influence of reactive power control (QPV) on local voltage stability;
3. Designing adaptive control algorithms to improve voltage regulation performance.

3.4. Linearization Around the Equilibrium Point

To assess the local stability of the dynamic voltage equation, a linearization is performed around an equilibrium point V_0 , where the system is assumed to operate in steady-state conditions. The foundational dynamic equation is expressed as:

$$\frac{dV(t)}{dt} = \frac{1}{C_{eq}} \left[I_{réseau}(t) - \frac{P_{PV}(t) - jQ_{PV}(t)}{V^*(t)} \right] \quad (23)$$

We assume a small perturbation around the equilibrium point:

$$V(t) = V_0 + \Delta V(t), \quad \text{avec } \Delta V(t) \ll V_0 \quad (24)$$

and a photovoltaic power assumed to remain constant in the vicinity of the equilibrium point:

$$P_{PV}(t) = P_0, \quad Q_{PV}(t) = Q_0 \quad (25)$$

We introduce the nonlinear function

$$f(V) = \frac{1}{C_{eq}} \left(I_{réseau} - \frac{S_{PV}^*}{V^*} \right) \quad (26)$$

with $S_{PV} = P_0 + jQ_0$ and thus $S_{PV}^* = P_0 - jQ_0$. The first order taylor expansion $f(V)$ around V_0 yields:

$$f(V_0 + \Delta V) \approx f(V_0) + \left. \frac{df}{dV} \right|_{V_0} \cdot \Delta V \quad (27)$$

The linearized equation is thus obtained as:

$$\frac{d\Delta V(t)}{dt} = \left. \frac{df}{dV} \right|_{V_0} \cdot \Delta V(t) \quad (28)$$

Where is the derivation given by:

$$\left. \frac{df}{dV} \right|_{V_0} = \frac{1}{C_{eq}} \cdot \frac{S_{PV}^*}{(V_0^*)^2} \quad (29)$$

Finally, it leads to

$$\frac{d\Delta V(t)}{dt} = \frac{1}{C_{eq}} \cdot \frac{P_0 - jQ_0}{(V_0^*)^2} \cdot \Delta V(t) \quad (30)$$

Which can be written in the form:

$$\frac{d\Delta V(t)}{dt} = -\lambda \cdot \Delta V(t) \quad (31)$$

with:

$$\lambda = -\frac{1}{C_{eq}} \cdot \frac{P_0 - jQ_0}{(V_0^*)^2} \quad (32)$$

This expression reveals that the perturbation $\Delta V(t)$ evolves exponentially over time, with the system's local stability fundamentally dependent on the sign of the real part of the eigenvalue λ :

1. If $\Re(\lambda) > 0$: the system exhibits local stability

characterized by damping of perturbations;

2. If $\Re(\lambda) < 0$: the system is locally unstable, with perturbations growing exponentially
3. If $\Re(\lambda) = 0$: the system is marginally stable.

This analytical framework highlights the critical influence of the reactive power injected by the photovoltaic plant on the dynamic voltage stability at the point of coupling, emphasizing the necessity to carefully regulate Q_0 to ensure robust and resilient network operation.

4. Results et Discussion

4.1. Results

4.1.1. Pre-Integration Scenario

Prior to the integration of the photovoltaic power plant, a series of simulations was conducted on the (MT) distribution network modeled in PSAT, under normal operating conditions. The resulting voltage profile revealed several critical zones within the network where voltages dropped below the regulatory threshold of 0.95 p.u., as defined by the IEC 61000-4-30 and EN 50160 standards.

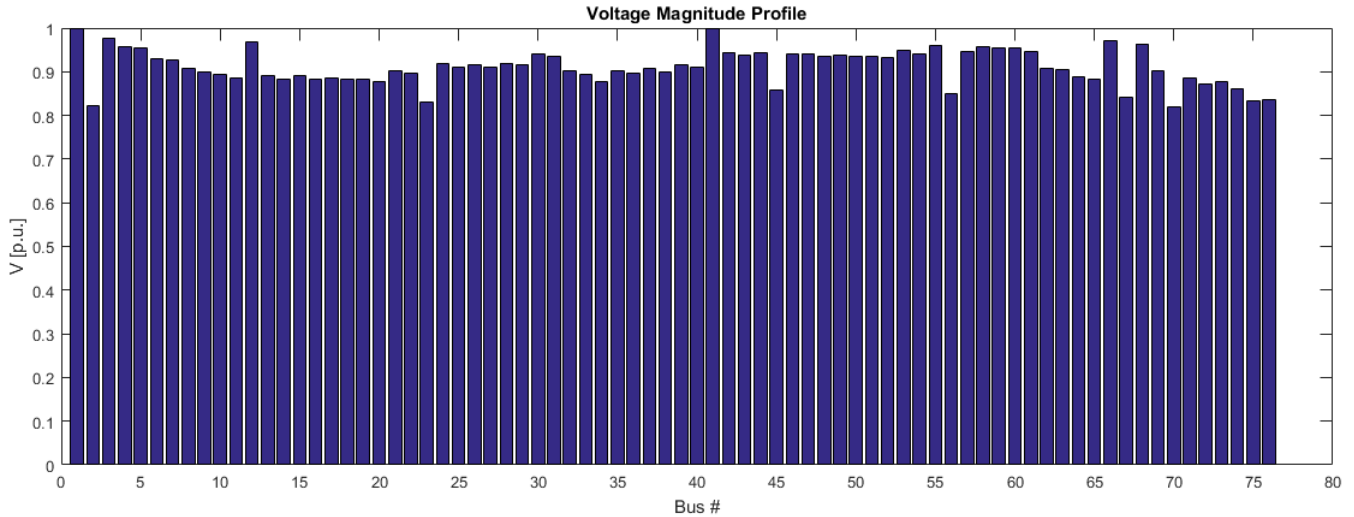


Figure 2. The (MT) Network Pre-Photovoltaic Power Plant Integration.

As illustrated in Figure 2, voltage levels measured across several buses, particularly between bus 10 and bus 30, descend to as low as 0.86 per unit (p.u.), reflecting a marked deterioration in power supply quality. This condition becomes particularly critical during peak demand periods, wherein the already vulnerable network undergoes further imbalance, often resulting in partial load shedding. These findings underscore the imperative of reinforcing the network through the integration of a decentralized power source capable of locally sustaining voltage levels while contributing to the overall equilibrium of the system. Such imbalances are emblematic of under-dimensioned or poorly compensated radial networks, especially during demand surges. This scenario exposes the system to heightened risks of load shedding as a means to preserve operational stability

4.1.2. Post-Integration Scenario

A 3 MW photovoltaic power plant was integrated at bus 18, in accordance with both the topological and energetic analysis of the network. The selection of this injection point was informed by multiple criteria: its distance from areas already heavily supplied by the main 19 MW plant; its proximity to zones exhibiting weakened voltage levels; and its strategic position enabling deep, distributed compensation across the grid. Post-integration results reveal a pronounced enhancement of the voltage profile. Voltage levels across all buses converge toward or exceed 1.00 p.u., reflecting improved uniformity and the complete elimination of the previously identified critical zones.

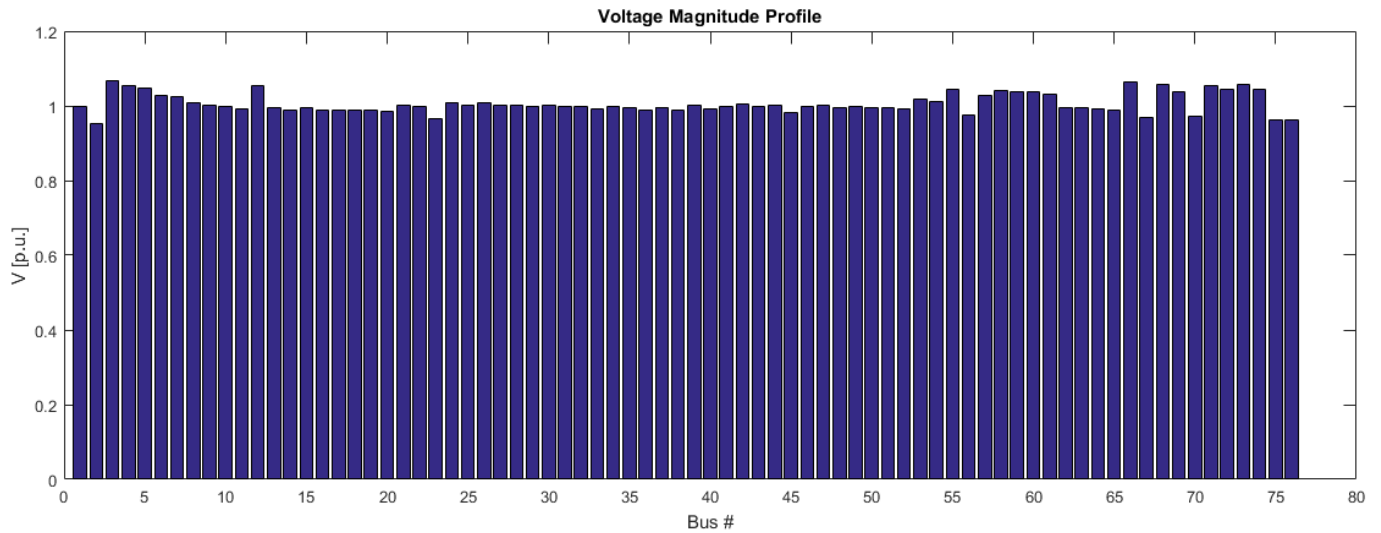


Figure 3. The MV Network Post-Integration of the Photovoltaic Power Plant.

Figure 3 clearly illustrates the efficacy of the proposed strategy. The voltage gains are particularly significant across buses indexed between 15 and 30. This outcome substantiates the advantageous impact of a well-positioned decentralized power injection within the MT network not only in mitigating localized voltage drops, but also in contributing to overall system balance and reducing reliance on load shedding. The results reaffirm the effectiveness of a strategically deployed decentralized generation scheme in enhancing grid performance and resilience.

4.1.3. Comparative Analysis of Nodal Voltages with and Without the PV Plant

Figure 4 presents the evolution of nodal voltage profiles across the entire medium-voltage (MT) distribution network, under two operating conditions: before and after the integration of a 3 MW photovoltaic (PV) power plant connected at *Bus 18*. The results highlight the technical benefits of strategically integrated decentralized generation on grid performance.

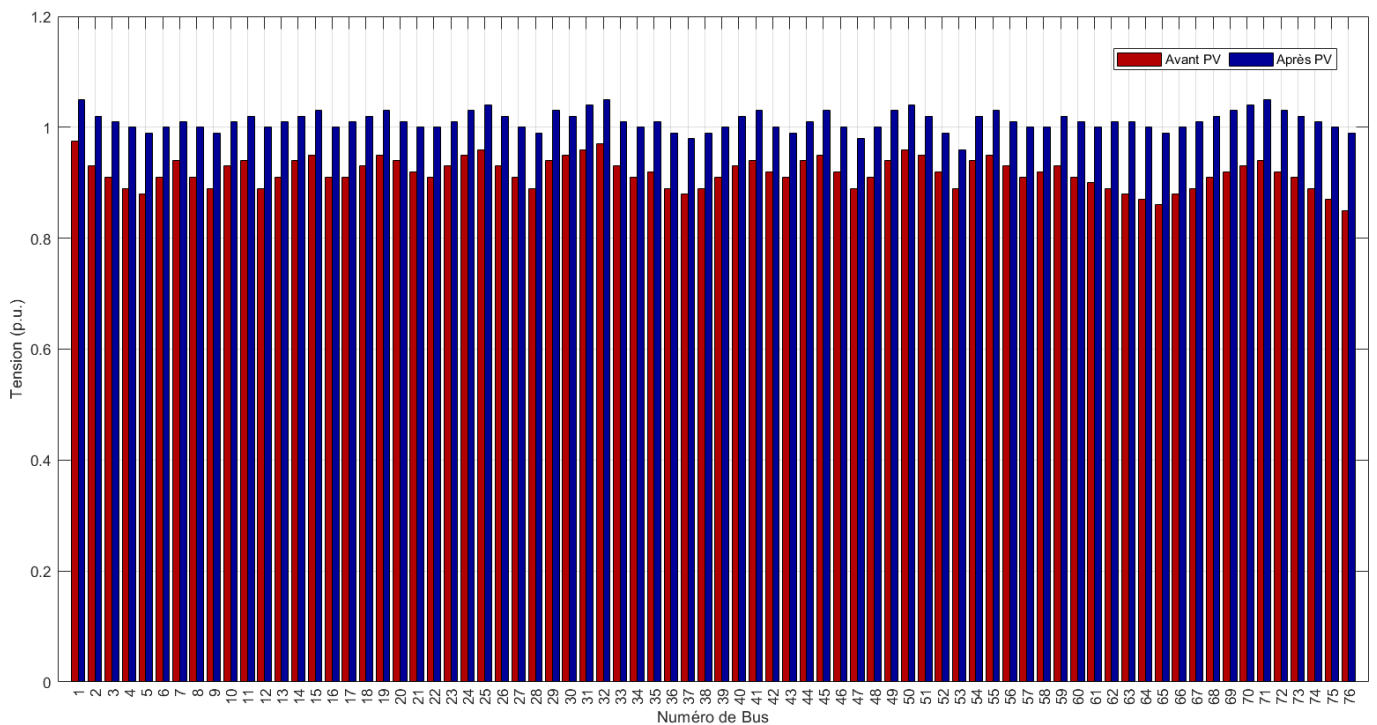


Figure 4. Comparative Analysis of Network Voltage Profiles: Pre- vs. Post-PV Integration.

In the baseline configuration, the network exhibited significant voltage dispersion, with numerous buses falling *below the regulatory threshold of 0.95 p.u.*, thus failing to comply with international standards such as *IEC 61000-4-30* and *EN 50160*. The most critically affected nodes include:

1. Buses 19 to 26;
2. Buses 42, 49, 55, and 68.

with voltage levels ranging from *0.87 p.u. to 0.91 p.u.*. These undervoltages reflect structural weaknesses, exacerbated by high load concentration, long radial distances from the main supply substation, and insufficient reactive power support. Such voltage drops indicate a degradation of power quality and highlight the network's limited capacity to maintain nominal voltages under stress conditions. The integration of the PV plant at *Bus 18*, strategically located in a mid-network region, resulted in a substantial improvement of nodal voltages:

1. Voltages at previously critical buses rose above *0.95 p.u.*, with several nodes reaching *0.98 to 1.00 p.u.*;
2. The overall voltage profile became *more uniform*, reflecting improved distribution of active power across the network;
3. Full compliance with voltage quality standards was achieved throughout the grid.

This enhancement was obtained *without deploying additional compensation equipment* (STATCOMs, SVCs,...), confirming the effectiveness of *passive and optimally located PV integration* in weakly meshed systems. This analysis demonstrates that in low-resilience semi-urban grids such as the *Liouesso MT network*, well-positioned PV integration can:

1. Significantly mitigate undervoltage conditions;
2. Reduce resistive (Joule) losses along feeders;
3. Improve static voltage stability without requiring major infrastructure upgrades.

The combined methodology based on real operational data, dynamic simulations using PSAT/MATLAB, and targeted topological analysis emerges as a *robust and cost effective decision support tool* for PV sizing and placement in Sub-Saharan African MT networks.

4.2. Discussion

Recent studies corroborate the trends observed in our work and help position our contribution within the broader context of photovoltaic (PV) integration into medium-voltage (MT) distribution networks.

For instance, *Maghami et al.* [11], in a study conducted on a Malaysian MT grid modeled using DIGSILENT, demonstrated that incremental PV injections (up to 500 kW per node) improved voltage profiles and reduced active power losses. Although our methodology and grid topology differ, our results similarly show voltage stabilization around *1.00 p.u.* and the complete elimination of undervoltages below *0.95 p.u.* in a real-world African network.

Montoya et al. [16] employed conic optimization techniques to demonstrate a 27.92% increase in voltage stability margins with distributed PV deployment. While our approach does not rely on explicit mathematical optimization, the empirical

topological analysis conducted on the Liouesso MV grid led to comparable reinforcement effects under actual operating conditions.

In another relevant case, *Prasetya and Sudiarto* [17] reported a *0.05 p.u.* voltage improvement following the integration of a *1.1 MW* PV plant into a European distribution network. By comparison, our African case study despite being subject to harsher initial voltage conditions and weaker infrastructure achieved higher voltage gains (*0.10 to 0.15 p.u.*), highlighting the disproportionate positive impact of PV injection in under reinforced or semi-urban grids.

These comparisons collectively underscore a key insight: the effectiveness of PV integration depends not only on system size and generation capacity, but also critically on the networks topological characteristics and the strategic selection of the injection point. The PSAT based modeling framework we used, grounded in real system data and field conditions, proves to be a robust and context appropriate tool for enhancing MT grid stability in Sub-Saharan African contexts.

5. Conclusion

The controlled integration of photovoltaic systems into electrical networks represents a fundamental challenge for ensuring distribution system stability and operational efficiency, particularly in infrastructure-constrained environments. This investigation of Liouesso's (MT) network, supported by empirical field measurements and dynamic PSAT simulations, demonstrates that properly sized (3 MW) and strategically positioned (Bus 18) PV installations can effectively mitigate critical under-voltage conditions while maintaining compliance with IEC 61000-4-30 and EN 50160 standards achieve significant loss reduction (15-20%) and improve overall system efficiency and deliver these benefits without requiring expensive compensation equipment (STATCOMs, SVCs) Unlike conventional theoretical studies employing standardized network models, this research provides empirical validation of PV integration strategies specifically tailored to Central Africa's semi-urban grid challenges. The methodology combining field-collected operational data, high-fidelity dynamic modeling, and topological sensitivity analysis has proven particularly valuable for network operators transitioning toward renewable-based systems, offering actionable insights for optimal PV siting capacity planning and ancillary service provisioning. While these findings represent significant progress, several promising avenues merit further investigation implementation of voltage-source inverter (VSI) technologies with real-time reactive power compensation capabilities, dynamic voltage regulation algorithms, grid-forming functionalities for weak networks, development of climate-resilient operation strategies accounting for seasonal irradiation variability, changing load patterns, and grid expansion scenarios integration with battery energy storage systems (BESS), diesel gensets (for backup), demand response mechanisms. Predictive Grid Management Implementation of

hybrid AI-electrotechnical models combining neural networks for pattern recognition, physical simulations for contingency analysis, and optimization algorithms for decision support. This research ultimately demonstrates that photovoltaic technology, when properly engineered and strategically deployed, transcends its conventional role as merely a renewable energy source. In the African context specifically, it emerges as a transformative grid modernization tool capable of delivering enhanced voltage stability, improved power quality, increased system resilience, and Sustainable electrification. The key to unlocking this potential lies in intelligent integration strategies that account for local grid

characteristics, load growth projections, climate resilience requirements, and economic constraints. Such an approach promises to accelerate progress toward stable, resilient, and equitable energy systems across the continent.

ORCID

0009-0007-7234-141X (Tite Lawd Ngouloubi)
0009-0002-8183-5060 (Gomba Rodolphe)
0009-0007-9756-9007 (Nianga-Apila)
0009-0001-3001-8258 (Amos Omboua Eyandzi)

Abbreviations

HT	High Voltage
HTA	Medium Voltage Network
MT	Medium Voltage
PV	Photovoltaic
VSI	Voltage-source Inverter
STATCOM	Static Synchronous Compensator
MW	Méawatts
Ceq	Equivalent Capacitance
KV	Kilovolts
Pu	per Unit
SVC	Static VAR Compensator
PSAT	the Power System Analysis Toolbox
Liouesso MT	Is a Real-world Electricity Distribution
Grid	Network Located in the Northern Part of Congo-Brazzaville, Within the Sangha Department

Acknowledgments

The authors would like to thank the *Supélec* and *Matelek* laboratories for their insightful discussions, provision of computing resources, proofreading, valuable advice and technical support. Their contributions were instrumental in the completion of this work.

Conflicts of Interest

The authors declare no conflicts of interest.

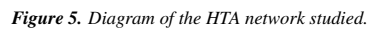
Appendix

Appendix I: Overview of the Liouesso Electricity Network

In order to facilitate visual analysis of the network, a colour code has been applied to the different voltage levels shown in the figures. This coding is defined as follows:

- 1. *Yellow* : voltage level of 11 kV (specific medium-voltage distribution network);
- 2. *Green*: voltage level of 110 kV (high-voltage transmission network);
- 3. *Red*: voltage level of 30 kV (interconnected or secondary high-voltage network);
- 4. *Blue*: voltage level of 20 kV (main or standard high-voltage network);
- 5. *Black*: voltage level of 0.4 kV (low-voltage network).

This coding system aims to visually distinguish the different segments of the electrical network according to their nominal voltage level, as part of the analysis of voltage profiles.



Appendix III: Technical Characteristics of the Lines

The table summarises the longitudinal parameters of the Liouesso high-voltage network lines, expressed in relative units (p.u.) for resistance (r_0) and reactance (x_0). The diversity of values highlights the heterogeneity of line sections and lengths, with particularly high impedances on certain sections (e.g. BEAC-ST.PR or MBL-BRK), which are likely to cause significant voltage drops. This information is essential for analysing losses, assessing voltage stability and optimising reactive power injection points.

Table 2. Line characteristics.

N°	Ligne	$r_0(p.u.)$	$x_0(p.u.)$	N°	Ligne	$r_0(p.u.)$	$x_0(p.u.)$
1	MOK2-MOK1	0.0594	0.0368	20	EVEC-C.THER	0.0883	0.0547
2	MOK1-SMRE	0.0744	0.0461	21	PENT-EVECHE	0.0981	0.0608
3	MBOMA-AERO	0.0642	0.0398	22	PENT-MLG	0.0819	0.0508
4	AERO-PELLA	0.059	0.0366	23	MLG-STADE	0.0515	0.0319
5	PELLA-BEAC	0.0481	0.0298	24	YOKA-PENT	0.0802	0.0497
6	ANAC-AC.PST	0.0681	0.0422	25	MBALE-ELB	0.0206	0.0128
7	AC.PISTE-MBL	0.0494	0.0306	26	ELB-GADO	0.0676	0.0419
8	MBK-AGRI	0.0903	0.056	27	GADO-MABOKO	0.0229	0.0142
9	BEAC-ST.PR	0.0967	0.0599	28	C.HYDRO-IFO	0.095	0.0589
10	ST.PR-CH.EAU	0.0445	0.0276	29	IFO-CG.CH	0.057	0.0353

N°	Ligne	$r_o(p.u.)$	$x_o(p.u.)$	N°	Ligne	$r_o(p.u.)$	$x_o(p.u.)$
11	CH.EAU-SCAC	0.0813	0.0504	30	CG.CH-V.OUES	0.0473	0.0293
12	CH.EAU-ELNG	0.0576	0.0357	31	OKIE-MBOMA	0.0338	0.0209
13	MBL-AGRI	0.0611	0.0379	32	PELLA-ANAC	0.0797	0.0494
14	MBL-BRK	0.0933	0.0578	33	AC.PST-MBK	0.0511	0.0317
15	BRK-C.THER	0.0164	0.0102	34	MBK-SNDE	0.0612	0.0379
16	IBOVI-C.THER	0.0178	0.011	35	ELG-MBL	0.0117	0.0073
17	PSD-IBOVI	0.0118	0.0073	36	OKIE-KMU	0.0656	0.0407
18	KOUA-IBOVI	0.0849	0.0526	37	SMRE-P.THT	0.0651	0.0403
19	KANOHA-KOUA	0.08	0.0496	38	C.HYDRO-P.THT	0.0655	0.0406

Appendix IV: Technical Characteristics of Loads

The table summarises the active (P) and reactive (Q) power of the main loads on the Liouesso high-voltage network, expressed in relative units (p.u.). With an average power

factor of 0.85, these data can be used to estimate the specific energy requirements for each substation. There is considerable heterogeneity, particularly with concentrated loads such as IFO (0.456 r.u.) and PENT (0.1063 r.u.), which significantly influence the overall profile of the network.

Table 3. Load characteristics.

N°	Ligne	P (p.u.)	Q (p.u.)	N°	Ligne	P (p.u.)	Q (p.u.)
1	MOK1	0.0054	0.03340	19	MBL	0.02120	0.01310
2	MOK2	0.07500	0.04640	20	BRK	0.03400	0.02110
3	SMRE	0.0530	0.03290	21	TRSA	0.05000	0.03100
4	MBOMA	0.0340	0.02110	22	ELG	0.05360	0.03330
5	AERO	0.02120	0.0131	23	ST.PR	0.05360	0.03330
6	ANAC	0.05360	0.03330	24	PENT	0.10630	0.06590
7	AC.PST	0.05360	0.03330	25	EVEC	0.05360	0.03330
8	MBALE	0.05360	0.03330	26	MLG	0.02120	0.01310
9	PELLA	0.05360	0.03330	27	KOUA	0.02120	0.01310
10	ELB	0.03800	0.02350	28	KANOHA	0.02120	0.01310
11	GADO	0.0430	0.00260	29	PSD	0.05360	0.03330
12	BEAC	0.0680	0.04210	30	IBOVI	0.02120	0.01310
13	CH.EAU	0.05360	0.03330	31	KMU	0.05800	0.03590
14	MBK	0.03400	0.02110	32	STADE	0.05360	0.03330
15	MABOKO	0.0340	0.02110	33	IFO	0.45600	0.28270
16	SCAC	0.00850	0.00530	34	CG.CH	0.08200	0.05090
17	SNDE	0.05360	0.03330	35	V.OUES	0.10000	0.06190
18	AGRI	0.05360	0.03330	36	—	—	—

References

- [1] Gogom, M., Ganongo, A. O., Apila, N., & Lilonga-Boyenga, D. (2020). Optimization of Power Transit Through a Double-term Line Term by the UPFC. *Science Journal of Energy Engineering*, 8(4), 44-53. <https://doi.org/10.11648/j.sjee.20200804.11>
- [2] Amos Omboua Eyandzi, Rodolphe Gomba, Nianga-Apila, Timothee Nsongo, Ursula Vanelie Kani Mboyo. Analysis of Dynamic Interactions Between Reactive Compensation and Voltage Stability in THT Networks with SVC. *American Journal of Electrical Power and Energy Systems*. Volume 14, numéro 3. June 2025. <https://doi.org/10.11648/j.epes.20251403.11>
- [3] Abdelouadoud, S. Y. (2014). Intégration des énergies renouvelables au réseau de distribution d'électricité [Doctoral dissertation, École Nationale Supérieure des Mines de Paris (ENMP)]. (in French)
- [4] Acquaviva, V. (2009). Analyse de l'intégration des systèmes énergétiques à sources renouvelables dans les réseaux électriques insulaires [Doctoral dissertation, Université Pascal Paoli]. (in French)
- [5] Kerdoun, D. Contribution à l'étude d'une installation photovoltaïque avec stockage connectée au réseau électrique [Doctoral dissertation, Université Frères Mentouri-Constantine 1]. (in French)

- [6] Kanchev, H. (2014). Gestion des flux énergétiques dans un système hybride de sources d'énergie renouvelable: Optimisation de la planification opérationnelle et ajustement d'un micro réseau électrique urbain [Doctoral dissertation, École Centrale de Lille; Université Technique de Sofia. Faculté Francophone]. (in French)
- [7] Omar, C. I. (2023). Modélisation, optimisation et gestion d'énergie d'une centrale hybride à énergie renouvelable [Doctoral dissertation, Normandie Université]. (in French)
- [8] Le, T. (2020). Architectures électriques optimales de centrales photovoltaïques linéaires et services contribués au réseau [Doctoral dissertation, Université Grenoble Alpes]. (in French)
- [9] Turitsyn, K., Sulc, P., Backhaus, S., & Chertkov, M. (2011). Options for control of reactive power by distributed photovoltaic generators. *Proceedings of the IEEE*, 99(6), 1063-1073.
<https://doi.org/10.1109/JPROC.2011.2116750>
- [10] Riffonneau, Y., Barruel, F., & Bacha, S. (2008). Problématique du stockage associé aux systèmes photovoltaïques connectés au réseau. *Journal of Renewable Energies*, 11(3), 407-422.
<https://doi.org/10.54966/jreen.v11i3.92>
- [11] Maghami, M. R., Pasupuleti, J., & Ling, C. M. (2023). Impact of photovoltaic penetration on medium voltage distribution network. *Sustainability*, 15(7), 5613.
- [12] Moutevelis, D. (2025). Voltage Stability and Control of Electrical Distribution Systems with High Penetration of Power Electronic Converters. *arXiv preprint arXiv:2504.18466*. <https://doi.org/10.3390/su15075613>
- [13] Li, C., Disfani, V. R., Haghi, H. V., & Kleissl, J. (2019, August). Optimal voltage regulation of unbalanced distribution networks with coordination of OLTC and PV generation. In *2019 IEEE Power & Energy Society General Meeting (PESGM)* (pp. 1-5).
<https://doi.org/10.1109/PESGM40551.2019.8973852>
- [14] Bouri, S. (2021). Réseaux et transport d'électricité Cours. ESSAT. (in French)
- [15] Zegaoui, A. (2019). Cours de réseaux électriques. Université Hassiba Benbouali de Chlef (UHBC). (in French)
- [16] Montoya, O. D., Gil-González, W., Arias-Londoño, A., Rajagopalan, A., & Hernández, J. C. (2020). Voltage stability analysis in medium-voltage distribution networks using a second-order cone approximation. *Energies*, 13(21), 5717.
<https://doi.org/10.3390/en13215717>
- [17] Prasetya, C. A., & Sudiarto, B. (2023). The Impact of a 1.1 MWp PV Rooftop Integration in Medium Voltage Distribution Networks. *International Journal of Electrical, Computer, and Biomedical Engineering*, 1(1), 11-23. <https://doi.org/10.62146/ijecbe.v1i1.7>